BIOINFORMATICS DISCOVERY NOTE Vol. 28 no. 10 2012, pages 1299–1302
doi:10.1093/bioinformatics/bts152

Structural bioinformatics

Advance Access publication March 30, 2012

Predicting giant transmembrane β-barrel architecture

Cyril F. Reboul[1,2], Khalid Mahmood[1,2], James C. Whisstock[1,2] and Michelle A. Dunstone[1,3,*]

[1]Department of Biochemistry and Molecular Biology, [2]ARC Centre of Excellence in Structural and Functional Microbial Genomics and [3]Department of Microbiology, Monash University, Clayton, VIC 3800, Australia

Associate Editor: Anna Tramontano

ABSTRACT

Motivation: The β-barrel is a ubiquitous fold that is deployed to accomplish a wide variety of biological functions including membrane-embedded pores. Key influences of β-barrel lumen diameter include the number of β-strands (n) and the degree of shear (S), the latter value measuring the extent to which the β-sheet is tilted within the β-barrel. Notably, it has previously been reported that the shear value for small antiparallel β-barrels ($n \leq 24$) typically ranges between n and $2n$. Conversely, it has been suggested that the β-strands in giant antiparallel β-barrels, such as those formed by pore forming cholesterol-dependent cytolysins (CDC), are parallel relative to the axis of the β-barrel, i.e. $S=0$. The $S=0$ arrangement, however, has never been observed in crystal structures of small β-barrels. Therefore, the structural basis for how CDCs form a β-barrel and span a membrane remains to be understood.

Results: Through comparison of molecular models with experimental data, we are able to identify how giant CDC β-barrels utilize a 'near parallel' arrangement of β-strands where $S=n/2$. Furthermore, we show how side-chain packing within the β-barrel lumen is an important limiting factor with respect to the possible shear values for small β-barrels ($n \leq 24$ β-strands). In contrast, our models reveal no such limitation restricts the shear value of giant β-barrels ($n > 24$ β-strands). Giant β-barrels can thus access a different architecture compared with smaller β-barrels.

Contact: michelle.dunstone@monash.edu

Supplementary information: Supplementary data are available at *Bioinformatics* online.

Received on January 26, 2012; revised on March 14, 2012; accepted on March 25, 2012

1 INTRODUCTION

The β-barrel structure is central to a large number of functionally diverse proteins. β-Barrels are deployed as enzymes [e.g. the outer membrane protease, OmpT (Vandeputte-Rutten *et al.*, 2001)], as water-soluble transport proteins [e.g. lipocalins (Breustedt *et al.*, 2005)], as fluorescent proteins [e.g. green fluorescent protein (Yang *et al.*, 1996)] and as membrane-embedded channels [e.g. porins (Weiss and Schulz, 1992)].

The properties of small β-barrels have been well-characterized. In particular, the shear value (S) of the β-barrel describes the stagger of individual β-strands. For a given number of β-strands (n), the greater the shear value, the greater the slope each β-strand is relative to the axis of the β-barrel lumen. Conversely, the lower the S-value, the closer to parallel the β-strand is relative to the axis of the β-barrel lumen (Supplementary Fig. S1). (A shear value of 0 results in β-strands that lie parallel to the barrel lumen.) Most importantly, when the number of β-strands and the shear value is known for a β-barrel, the diameter can be calculated for cylindrical β-barrels with a high degree of accuracy (McLachlan, 1979; Murzin *et al.*, 1994a).

For small β-barrels ($n \leq 24$) that are structurally characterized, the S-value of these structures lies between n and $2n$ (Murzin *et al.*, 1994b; Nagano *et al.*, 1999; Schulz, 2002). To date, the structures of over 190 transmembrane β-barrels have been determined (Fairman *et al.*, 2011); analysis of these data reveal that membrane β-barrels obey the same structural rules observed for their soluble counterparts. A subset of transmembrane β-barrels includes structures that are formed by homo-oligomerization. Examples of such β-barrels include TolC (Koronakis *et al.*, 2000) and β-pore forming toxins such as α-haemolysin (Song *et al.*, 1996).

Although membrane β-barrels have contributed to our understanding of small β-pore forming toxins, less is known about the giant homo-oligomeric β-barrel pores formed by members of the cholesterol-dependent cytolysins (CDC)/Membrane Attack Complex/Perforin (MACPF) superfamily (Hotze and Tweten, 2011; Rosado *et al.*, 2008). This superfamily includes key bacterial virulence factors produced by Gram positive bacteria as well as the major immune effectors of mammals (Kondos *et al.*, 2010). No crystal structure of a MACPF or CDC pore has been determined to date, however, the 28 Å resolution cryo-electron microscopy (EM) structure of pneumolysin reveals that this CDC forms a giant 240 Å diameter β-barrel that contains 38 monomers (Tilley *et al.*, 2005). To make this β-barrel, each pneumolysin monomer contributes two amphipathic β-hairpins, i.e. four antiparallel β-strands (Shatursky *et al.*, 1999; Shepard *et al.*, 1998).

Initial models presented through EM studies of the CDC, pneumolysin, suggested that the β-strands are parallel to the lumen in order to reach and fully span the lipid bilayer as a β-barrel (Tilley *et al.*, 2005). However, such an arrangement would not be consistent with a shear value between n and $2n$ as observed in the known crystal structures of transmembrane β-barrels (Pali and Marsh, 2001; Schulz, 2002). Here, using molecular models, we show that the optimal shear value of these giant β-barrel structures is $S=n/2$, i.e. arranged in a near parallel fashion with respect to the β-barrel lumen. We further demonstrate that β-barrels with <24 β-strands are unable to readily access such architecture as a consequence of luminal side-chain packing constraints.

*To whom correspondence should be addressed.

2 METHODS

2.1 β-Barrel parameter refinement

To build atomic models of β-barrels, an initial Cα template geometry was generated based on known β-barrel structures (McLachlan, 1979; Murzin *et al*., 1994a). For a given pair of n and S, idealized cylindrical β-barrels were built with a radius R and a β-strand slope of α with respect to the cylinder axis, following McLachlan (1979) and in a fashion reminiscent of research by Sansom and Kerr (1995). Each residue is represented by its Cα and placed on the surface of the cylinder. Positions of the Cα are fully determined by the values of n and S and by the choice of the grid parameters a and b (Murzin *et al*., 1994a). a is the Cα–Cα distance between adjacent residues on the same β-strand (intra-strand), while b is the Cα–Cα distance across hydrogen-bonded β-strands (inter-strand).

When building such β-barrels, the values of the parameters a and b influence the local (e.g. intra- and inter-strand distances) as well as global (e.g. radius) structural features of the resulting models. In this study, we optimized the a and b parameters using a training set of antiparallel membrane-embedded β-barrels that are formed by homo-oligomers. We searched protein structure databases using the MPtopo and PDBe tools (Jayasinghe *et al*., 2001; Velankar *et al*., 2011) and found eight suitable structures following these strict criteria. Of these eight chosen structures (Supplementary Table S1), the transmembrane β-barrels were isolated and their Cα coordinates projected on the surface of a fitted cylinder (based on least-square fitting) and the grid parameters were derived. All structures showed a clear cylindrical and symmetric shape and our analysis found that $a = 3.48$ Å and $b = 4.83$ Å. The latter values are found to be in very good agreement with previously reported ones for antiparallel water-soluble β-barrels ($a = 3.53$ Å; $b = 4.87$ Å) (Chou and Scheraga, 1982). The ratio $a/b = 0.721$ is also in excellent agreement with the 0.719 reported for a non-overlapping set of transmembrane β-barrels (Pali and Marsh, 2001).

Using these refined parameters, the β-barrel Cα scaffold was built: first the Cα (β-strand 1) is placed at a distance R to the arbitrary cylinder axis. The Cα of the next residue is then positioned at a distance a on the cylinder surface such that the angle between the Cα–Cα vector and the β-barrel axis is α. The remaining residues of the β-strand are iteratively positioned the same way. The first Cα of the adjacent β-strand (strand 2) is positioned on the cylinder surface, at a distance b from an adjacent Cα belonging to β-strand 1 in such a way that the Cα–Cα vector is perpendicular to β-strand 1. The other residues of β-strand 2 are placed as was done for β-strand 1. The remaining β-strands are built iteratively using the same method.

2.2 Atomistic β-barrel models

Based on the Cα scaffold, full atomistic models were first built as poly-alanine β-strands. The Cβ atoms were positioned 1.5 Å apart from the Cα alternately facing towards the pore lumen and towards the membrane, thus ensuring proper orientation of the side chains and the antiparallel nature of the β-barrels. Amino acid sequences of the β-hairpins and β-turns were subsequently mapped onto this framework using MODELLER (Eswar *et al*., 2006). The resulting structures were subjected to three cycles of energy minimization employing NAMD 2.8 (Phillips *et al*., 2005), the CHARMM22 forcefield with CMAP correction (MacKerell *et al*., 1998; Mackerell *et al*., 2004) and the GBIS solvent model (Tanner *et al*., 2011). In the first step, harmonic restraints on heavy atoms are smoothly relaxed from 200 to 5 kJ (mol Å)$^{-1}$ to resolve potential steric clashes. In the second step, inter-strand backbone hydrogen bonds constraints are employed (N–H…O=C) with a reference value of 1.9 Å (McLachlan, 1979) and relaxed from 5 to 1 kJ (mol Å)$^{-1}$. The hydrogen bonds correspond to the canonical antiparallel β-strand hydrogen bonding pattern. In the final step, all constraints are relaxed. Energy minimizations involved 15 000 steps in total.

Based on the values of n and S in our dataset, the corresponding β-barrels atomic models were built and found to reproduce closely the crystallographic structure with an average Cα RMSD ~1.1 Å (Supplementary Table S1), thus validating our approach and methodology. Model pore radii were found to be in excellent agreement with radii calculated from the X-ray structures.

Transmembrane β-barrel models were subsequently built for pneumolysin (38 subunits; $n = 152$) (Tilley *et al*., 2005). Five models were built with shear values $S = 0, n/2, n, 3n/2$ and $2n$. In addition, the estimate of error of β-barrel diameter estimation is calculated (see Supplementary Materail).

2.3 Side-chain packing in the β-barrel interior

To probe the influence of side-chain packing on β-barrel architecture (e.g. the choice of S given n), we positioned pseudo-side chains in the β-barrel interior of our Cα scaffold and calculated the van der Waals (vdW) interaction energy (E_{vdW}) of one pseudo-side chain with its closest eight neighbours (Supplementary Fig. S2). To achieve this, a pseudo-methyl group per residue was positioned in the β-barrel interior 3.0 Å away from the Cα, thus mimicking an amino acid side chain with an aliphatic group at position Cγ. As a result, a methyl group is placed in the interior every second residue (i.e. following the alternate orientation of side chains in β-strands). The resulting semi-quantitative E_{vdW} calculated for each combination of (n, S) are presented in Figure 2 and compared with known structures (Supplementary Table S2). Methyl group vdW parameters were taken from the GROMOS forcefield (Oostenbrink *et al*., 2004).

3 RESULTS

3.1 Predicting shear values of CDC β-barrels

The 28 Å resolution cryo-EM structure of pneumolysin contains 152 β-strands and forms a pore 240 Å in diameter [PLY; EMDB ID: EMD-1107 (Tilley *et al*., 2005)]. We compared a range of models and identified the β-barrel with a shear value that most closely agreed with these experimental data. Homo-oligomeric antiparallel β-barrels typically have an S-value that is an integer multiple of the number of β-strands, therefore, $S = n$ and $S = 2n$ models were built together with the $S = 0$ model. Moreover, since two hairpins (i.e. four β-strands) are contributed per monomer, it is possible for CDC β-barrels to have shear values of $S = n/2$ or $S = 3n/2$ (Supplementary Fig. S1).

The model that fitted best within the experimental EM data, based upon predicted radius, possessed a shear value of $S = n/2$ (Fig. 1, Supplementary Table S3). Furthermore, our analysis suggests that a β-barrel with $S = n/2$ would also permit a right-handed twist of the β-strands that is characteristic of β-barrels formed by L-amino acids.

Given the 28 Å resolution of the EM data, however, the model with $S = 0$ may be possible. Neither the $S = 0$ nor the $S = n/2$ model can be favoured in terms of the overall height of the β-barrels with respect to the position of the CDC globular head domain since there is only a 7 Å reduction in height between the $S = 0$ and the $S = n/2$ models (over a total distance of 88 Å). In both models, the globular head domains can fit well within the density (Fig. 1B).

In contrast, S-values of n, $3n/2$ or $2n$ resulted in pore sizes that are far larger than the observed dimensions of the pore (Fig. 1). Importantly, the calculated minimum diameter for the $S = n$ model and the calculated maximum diameter for the $S = n/2$ model do not overlap (Supplementary Table S3). The minimum diameter for the $S = n$ model does not overlap with the EM density of the β-barrel. We were, therefore, confident in ruling out the $S = n$ model for this CDC.

Perfringolysin O (PFO), while it has no 3D EM data of the pore, has contributed to our understanding of the mechanism of CDC pore formation (Rossjohn *et al*., 1997; Shatursky *et al*., 1999; Shepard *et al*., 1998). Importantly, pyrene labelling studies of adjacent side

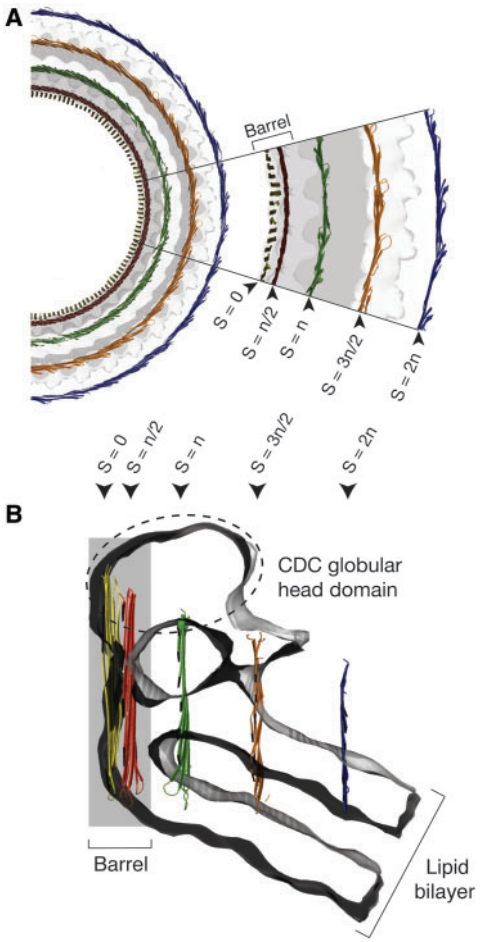

Fig. 1. Superposition of the pneumolysin 38-mer pore with atomic pore models of various shear (S) values. (**A**) Top view. Left: models and 3D-EM map; right: models with shear values indicated by arrows. (**B**) Blow-out view. The S-values presented are: 0 (yellow), $n/2$ (76; red), n (152; green), $n/2$ (228; orange) and $2n$ (304; blue).

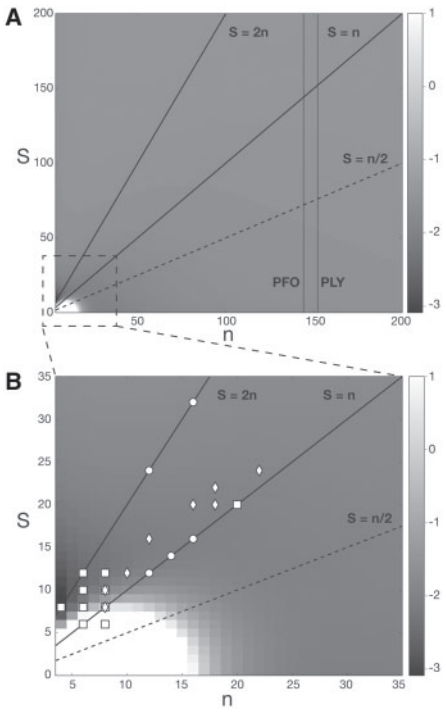

Fig. 2. Interior side-chain packing as a function of β-barrel architecture. In (**A**) and (**B**), the interior side-chain packing is semi-quantitatively estimated by side-chain van der Waals energies (in kJ mol^{-1}). White regions ($E_{vdW} > 1.0$ kJ mol^{-1}) are considered unfavourable, grey regions ($E_{vdW} < 1.0$ kJ mol^{-1}) are considered favourable. Squares represent water-soluble β-barrels, diamonds represent membrane β-barrels and circles represent oligomeric antiparallel membrane β-barrels.

chains in PFO suggest that the β-strands are slightly staggered and, therefore, favour the slightly tilted $S = n/2$ model over the parallel $S = 0$ model (Ramachandran *et al.*, 2004; Supplementary Fig. S3).

3.2 Constraints governing β-barrel size and shape

For small β-barrels ($n < 24$) the shear value lies within the $n \leq S \leq 2n$ range (Murzin *et al.*, 1994b; Nagano *et al.*, 1999; Schulz, 2002). We, therefore, investigated whether there were any constraints that limited the S-value for a given number of β-strands.

A major constraint for small β-barrel architecture is the packing of the side chains in the interior of the β-barrel (Lesk *et al.*, 1989; Murzin *et al.*, 1994a). Typically, β-sheets in water-soluble β-barrels bury hydrophobic residues in the interior. In contrast, in membrane-embedded pores, the interior channel is lined with hydrophilic residues, whereas the exterior surface of the β-barrel is hydrophobic. The packing of the side chains in the lumen of the β-barrel plays an important role in the overall architecture of the β-barrel.

We calculated the theoretical side-chain van der Waals energies for all theoretical combinations of S and n in antiparallel β-barrels (Fig. 2). It can be predicted from the plot that it is not energetically favourable for small antiparallel β-barrels to achieve $0 \leq S \leq n$ structural arrangement due to steric clashes made by the lumen-orientated side chains. However, side-chain packing no longer becomes a constraint for β-barrel architecture in β-barrels >20 β-strands. Therefore, giant β-barrels formed by CDCs are capable of forming 'near parallel' barrels, whereas small β-barrels are not.

3.3 Validation of the side-chain constraints for small soluble β-barrels

To validate the side-chain packing plot (Fig. 2), we analysed the range in known structures of both soluble β-barrels and membrane-embedded β-barrel solved to date. Most structures lie within the energetically favourable region of the plot (Fig. 2B, Supplementary Table S2). In addition, the structures in general lie within the $n \leq S \leq 2n$ (Murzin *et al.*, 1994b; Nagano *et al.*, 1999; Schulz, 2002) region.

There are two known exceptions to this rule: the first is oxidoreductase (PDB ID 3sod), which has eight β-strands and a shear value of 6 ($n = 8$, $S = 6$) and thus lying within the energetically unfavourable region. However, oxidoreductase has only a single hydrogen bond between two of the β-strands due to the constraints

of the β-sheet and the stacking of side chains within the β-barrel and thus resembles a 'burst' or overstuffed β-barrel (Supplementary Fig. S4). The second β-barrel type lies in the unfavourable region is tetrahydrodipicolinate N-succinyltransferase ($n=6$, $S=6$) (PDB ID 1tdt). This is a very short β-barrel that contains only a single side chain per β-strand stacked inside the β-barrel lumen (Supplementary Fig. S5). Lumen-directed side chains in this structure can, therefore, readily access space at the top and the bottom of the β-barrel.

Together, these exceptions support the idea that steric clashes in the interior of β-barrels affect the possible combinations of shear (S) and β-strand number (n) in small antiparallel 'near-ideal' β-barrels that contain extensive β-sheet hydrogen bonds between all β-strands.

It is also important to note that our calculations suggest that the constraints imposed by side chains on the S to n ratio disappear as β-barrel sizes grow over 20 β-strands. For giant β-barrels such as CDC pore forming proteins, it is predicted that there are no limitations to the S/n ratio imposed by luminal side-chain packing. In summary, our data show that, as β-barrels grow larger, the interior lumen becomes less curved and more amenable to a smaller shear to number of β-strands ratio.

4 DISCUSSION

Comparison of β-barrel models with published 3D-EM structures (Tilley *et al*., 2005), reveals that for CDCs, a β-barrel formed with a shear value of $S=n/2$ provides the best fit. This is supported by the biophysical research performed upon PFO (Ramachandran *et al*., 2004). We further found that giant β-barrels have no apparent limitation with respect to shear values. In contrast, the architecture of smaller β-barrels is severely constrained by lumen side-chain packing. To the best of our knowledge, β-barrels that are long enough to span a membrane and possess a shear value of $S=n/2$ or 0 have not been observed at atomic resolution. However, our data lend support to the idea that CDCs can indeed form such structures. These ideas may be of further utility in modelling large β-barrels formed by other supermolecular complexes.

ACKNOWLEDGEMENTS

The authors thank Helen Saibil, Rodney Tweten and Bosco Ho for helpful discussions.

Funding: Australian Research Council [DP0986811, FF0883418 to J.C.W.]; National Health and Medical Research Council [606471 to M.A.D.]; and C.F.R. is supported by the Australian Postgraduate Award.

Conflict of Interest: none declared.

REFERENCES

Breustedt,D.A. *et al.* (2005) The 1.8–A crystal structure of human tear lipocalin reveals an extended branched cavity with capacity for multiple ligands. *J. Biol. Chem.*, **280**, 484–493.

Chou,K.C. and Scheraga,H.A. (1982) Origin of the right-handed twist of beta-sheets of poly(LVal) chains. *Proc. Natl Acad. Sci. USA*, **79**, 7047–7051.

Eswar,N. *et al.* (2006) Comparative protein structure modeling using Modeller. *Curr. Protoc. Bioinformatics*, **Chapter 5**, Units 5–6.

Fairman,J.W. *et al*. (2011) The structural biology of β-barrel membrane proteins: a summary of recent reports. *Curr. Opin. Struct. Biol.*, **21**, 523–531.

Hotze,E.M. and Tweten,R.K. (2012) Membrane assembly of the cholesterol-dependent cytolysin pore complex. *Biochim. Biophys. Acta.*, **1818**, 1028–1038.

Jayasinghe,S. *et al*. (2001) MPtopo: a database of membrane protein topology. *Protein Sci.*, **10**, 455–458.

Kondos,S.C. *et al.* (2010) The structure and function of mammalian membrane-attack complex/perforin-like proteins. *Tissue Antigens*, **76**, 341–351.

Koronakis,V. *et al.* (2000) Crystal structure of the bacterial membrane protein TolC central to multidrug efflux and protein export. *Nature*, **405**, 914–919.

Lesk,A.M. *et al.* (1989) Structural principles of alpha/beta barrel proteins: the packing of the interior of the sheet. *Proteins*, **5**, 139–148.

MacKerell,A.D. *et al.* (1998) All-atom empirical potential for molecular modeling and dynamics studies of proteins. *J. Phys. Chem. B*, **102**, 3586–3616.

Mackerell,A.D.,Jr. *et al.* (2004) Extending the treatment of backbone energetics in protein force fields: limitations of gas-phase quantum mechanics in reproducing protein conformational distributions in molecular dynamics simulations. *J. Comput. Chem.*, **25**, 1400–1415.

McLachlan,A.D. (1979) Gene duplication in the evolution of the yeast hexokinase active site. *Eur. J. Biochem.*, **100**, 181–187.

Murzin,A.G. *et al.* (1994a) Principles determining the structure of beta-sheet barrels in proteins. I. A theoretical analysis. *J. Mol. Biol.*, **236**, 1369–1381.

Murzin,A.G. *et al.* (1994b) Principles determining the structure of beta-sheet barrels in proteins. II. The observed structures. *J. Mol. Biol.*, **236**, 1382–1400.

Nagano,N. *et al.* (1999) Barrel structures in proteins: automatic identification and classification including a sequence analysis of TIM barrels. *Protein Sci.*, **8**, 2072–2084.

Oostenbrink,C. *et al.* (2004) A biomolecular force field based on the free enthalpy of hydration and solvation: the GROMOS force-field parameter sets 53A5 and 53A6. *J. Comput. Chem.*, **25**, 1656–1676.

Pali,T. and Marsh,D. (2001) Tilt, twist and coiling in beta-barrel membrane proteins: relation to infrared dichroism. *Biophys. J.*, **80**, 2789–2797.

Phillips,J.C. *et al.* (2005) Scalable molecular dynamics with NAMD. *J. Comput. Chem.*, **26**, 1781–1802.

Ramachandran,R. *et al.* (2004) Membrane-dependent conformational changes initiate cholesterol-dependent cytolysin oligomerization and intersubunit beta-strand alignment. *Nat. Struct. Mol. Biol.*, **11**, 697–705.

Rosado,C.J. *et al.* (2008) The MACPF/CDC family of pore-forming toxins. *Cell.Microbiol.*, **10**, 1765–1774.

Rossjohn,J. *et al.* (1997) Structure of a cholesterol-binding, thiol-activated cytolysin and a model of its membrane form. *Cell*, **89**, 685–692.

Sansom,M.S. and Kerr,I.D. (1995) Transbilayer pores formed by beta-barrels: molecular modeling of pore structures and properties. *Biophys. J.*, **69**, 1334–1343.

Schulz,G.E. (2002) The structure of bacterial outer membrane proteins. *Biochim. Biophys. Acta.*, **1565**, 308–317.

Shatursky,O. *et al.* (1999) The mechanism of membrane insertion for a cholesterol-dependent cytolysin: a novel paradigm for pore-forming toxins. *Cell*, **99**, 293–299.

Shepard,L.A. *et al.* (1998) Identification of a membrane-spanning domain of the thiol-activated pore-forming toxin *Clostridium perfringens* perfringolysin O: an alpha-helical to beta-sheet transition identified by fluorescence spectroscopy. *Biochemistry*, **37**, 14563–14574.

Song,L. *et al.* (1996) Structure of staphylococcal α-hemolysin, a heptameric transmembrane pore. *Science*, **274**, 1859–1865.

Tanner,D.E. *et al.* (2011) Parallel generalized born implicit solvent calculations with NAMD. *J. Chem. Theory Comput.*, **7**, 3635–3642.

Tilley,S.J. *et al.* (2005) Structural basis of pore formation by the bacterial toxin pneumolysin. *Cell*, **121**, 247–256.

Vandeputte-Rutten,L. *et al.* (2001) Crystal structure of the outer membrane protease OmpT from Escherichia coli suggests a novel catalytic site. *EMBO J.*, **20**, 5033–5039.

Velankar,S. *et al.* (2012) PDBe: protein data bank in Europe. *Nucleic Acids Res.*, **40**, D445–452.

Weiss,M.S. and Schulz,G.E. (1992) Structure of porin refined at 1.8 A resolution. *J. Mol. Biol.*, **227**, 493–509.

Yang,F. *et al.* (1996) The molecular structure of green fluorescent protein. *Nat. Biotechnol.*, **14**, 1246–1251.